PCP
PLANT & CELL PHYSIOLOGY

JOINTLESS Maintains Inflorescence Meristem Identity in Tomato

Samuel Huerga-Fernández[1], Nathalie Detry[1], Beata Orman-Ligeza[1], Frédéric Bouché[1,2], Marc Hanikenne[2] and Claire Périlleux[1,*]

[1]Laboratory of Plant Physiology, InBioS—PhytoSYSTEMS, Department of Life Sciences, University of Liège, Chemin de la Vallée, 4, Liège B-4000, Belgium
[2]Laboratory of Plant Translational Biology, InBioS—PhytoSYSTEMS, Department of Life Sciences, University of Liège, Chemin de la Vallée, 4, Liège B-4000, Belgium

*Corresponding author: E-mail, cperilleux@uliege.be

(Received 23 January 2024; Accepted 17 April 2024)

***JOINTLESS* (*J*) was isolated in tomato (*Solanum lycopersicum*) from mutants lacking a flower pedicel abscission zone (AZ) and encodes a MADS-box protein of the SHORT VEGETATIVE PHASE/AGAMOUS-LIKE 24 subfamily. The loss of *J* function also causes the return to leaf initiation in the inflorescences, indicating a pivotal role in inflorescence meristem identity. Here, we compared *jointless* (*j*) mutants in different accessions that exhibit either an indeterminate shoot growth, producing regular sympodial segments, or a determinate shoot growth, due to the reduction of sympodial segments and causal mutation of the *SELF-PRUNING* (*SP*) gene. We observed that the inflorescence phenotype of *j* mutants is stronger in indeterminate (*SP*) accessions such as Ailsa Craig (AC), than in determinate (*sp*) ones, such as Heinz (Hz). Moreover, RNA-seq analysis revealed that the return to vegetative fate in *j* mutants is accompanied by expression of *SP*, which supports conversion of the inflorescence meristem to sympodial shoot meristem in *j* inflorescences. Other markers of vegetative meristems such as *APETALA2c* and branching genes such as *BRANCHED 1* (*BRC1a/b*) were differentially expressed in the inflorescences of *j*(AC) mutant. We also found in the indeterminate AC accession that *J* represses homeotic genes of B- and C-classes and that its overexpression causes an oversized leafy calyx phenotype and has a dominant negative effect on AZ formation. A model is therefore proposed where *J*, by repressing shoot fate and influencing reproductive organ formation, acts as a key determinant of inflorescence meristems.**

Keywords: Abscission ● Branching ● Flower development ● Inflorescence ● *Solanum lycopersicum* ● Tomato

Introduction

Loss of seed dispersal is a major trait of flowering plant domestication, as it avoids yield losses before harvest. In the fleshy fruit species tomato (*Solanum lycopersicum*), fruit drop occurs by fracture across an abscission zone (AZ) in the middle of the pedicel. The formation of this boundary, made of layers of dense and small cells, starts at an early stage of flower development, when sepals are being initiated (Tabuchi et al. 2000). Lack of AZ, described as a 'jointless' phenotype, has thus been selected by breeders as a desirable trait, which in addition to preventing fruit drop facilitates harvest (Bergougnoux 2014). Causative mutations were found in two MADS-box protein-encoding genes, *JOINTLESS* (*J*) and *JOINTLESS 2* (*J2*), which fall in the *SHORT VEGETATIVE PHASE/AGAMOUS-LIKE 24* (*SVP/AGL24*) and *SEPALLATA* (*SEP*) subfamilies identified in *Arabidopsis*, respectively (Mao et al. 2000, Zhang et al. 2000, Gomez-Roldan et al. 2017, Soyk et al. 2017). Consistent with the fact that the AZ is formed at the sepal initiation stage, a mutation in the *MACROCALYX* (*MC*) gene, which is orthologous to *APETALA 1* (*AP1*), affects sepal identity and causes abnormal AZ (Shalit et al. 2009, Yuste-Lisbona et al. 2016). At the molecular level, binary interactions between J, J2 and MC proteins were found (Nakano et al. 2012, Liu et al. 2014), and it was thus hypothesized that these MADS-box proteins form a multimeric complex activating the formation of flower AZ. Transcriptomic analyses showed that, downstream of this trigger, the expression of meristem and boundary genes such as *BLIND* (*Bl*), *WUSCHEL* (*SlWUS*), *GOBLET* (*GOB*) and *LATERAL SUPPRESSOR* (*Ls*) is specifically activated in the pre-abscission AZ but not in other pedicel tissues (Nakano et al. 2012, Liu et al. 2014, Gomez-Roldan et al. 2017).

Plant Cell Physiol. 00(00): 1–15 (2024) doi:https://doi.org/10.1093/pcp/pcae046, Advance Access publication on 18 April 2024, available online at https://academic.oup.com/pcp

Although mutations in *J* or *J2* suppress the pedicel AZ, only *j2* was introduced in breeding programs because the *j* mutation causes another, undesirable, phenotype. Indeed, tomato plants deficient in *J* function bear inflorescences that return to leaf initiation after having formed a few flowers, which negatively impacts fruit yield (Butler 1936, Philouze 1978, Quinet et al. 2006, Szymkowiak and Irish 2006, Thouet et al. 2012). From a fundamental point of view, this floral reversion suggests that the *J* gene might establish a key link between AZ formation and inflorescence meristem fate.

Flowering in tomato starts with a switch in the fate of the shoot apical meristem (SAM), which first undergoes an intermediate stage characterized by typical doming, and then terminates into a flower meristem (FM). At the same time, a lateral inflorescence meristem, called 'sympodial inflorescence meristem' (SIM) because of its lateral origin, emerges on the flank of the FM and itself progresses toward FM fate, while a second SIM is initiated on its flank. This process follows an iterative sympodial pattern and builds a monochasial cyme (Castel et al. 2010). While the SAM elaborates the first inflorescence, shoot growth is continued by the axillary meristem hosted by the uppermost leaf. This axillary meristem, called sympodial shoot meristem (SYM), is maintained vegetative by the expression of a repressor of flowering, *SELF-PRUNING* (*SP*), which is orthologous to *TERMINAL FLOWER 1* in *Arabidopsis* (Pnueli et al. 1998). Outgrowth of the SYM occurs as the expression of *SP* diminishes (Thouet et al. 2008) until the SYM enters the floral transition itself and is relayed by a second SYM. The tomato shoot is thus composed of an 'initial' segment formed by the SAM, whose size depends on the duration of the vegetative phase of the plant, and of successive sympodial shoot segments, usually made of three leaves each. This sympodial shoot growth is virtually infinite in cultivars expressing *SP*, which are 'indeterminate'. By contrast, cultivars carrying an *sp* mutation stop growing after a few reduced sympodial segments, producing short and bushy 'determinate' plants (Pnueli et al. 1998).

The size and the architecture of the tomato inflorescence depend on the spatio-temporal regulation of the individual meristems that build it and develop in very close vicinity (Périlleux and Huerga-Fernández 2022). Most importantly, the identity of the SIM requires that this meristem has reproductive competence but does not progress too fast toward FM fate. Indeed, accelerated development might lead to solitary flower phenotypes as it was observed e.g. when the FM identity genes *FALSIFLORA* (*FA*) or *ANANTHA* (*AN*) were over- or heterochronically expressed (MacAlister et al. 2012). On the opposite, delayed expression of *FA* or *AN* leads to the proliferation of SIMs and increased inflorescence branching, as observed in the *compound inflorescence* (*s*) mutant (Lippman et al. 2008). It was inferred from these observations that meristem maturation is a gradual process defined molecularly by dynamic gene expression and that its rate affects the architecture of the inflorescence: the slowest the maturation rate, the most branched the inflorescence (Park et al. 2012). We previously hypothesized that the *J* gene plays a role in this network because its loss of function suppresses the highly branched phenotype of *s* mutant and hence supposedly compensates for its meristem maturation default (Thouet et al. 2012, Périlleux et al. 2014). This hypothesis, however, remained to be tested and to be reconciled with the fact that *j* mutation also causes the return of SIMs to vegetative functioning.

In order to further explore the biological function of *J* in the elaboration of the inflorescence in tomato, we performed and report here RNA-seq analyses of *J* loss-of-function and overexpressing plants.

Results

Inflorescence phenotypes of *j* mutants

The original *j* mutant described by Butler (1936) was in an indeterminate (*SP*/*SP*) background and, in addition to the lack of AZ, showed reversion of the inflorescences back to vegetative development after the initiation of few flowers. Later studies showed that these two morphological traits of *j* mutants could not be separated, but that inflorescences differed among indeterminate and determinate (*sp*/*sp*) varietal backgrounds (Emery and Munger 1970). We therefore performed a side-by-side comparison of different *j* mutants: two in an indeterminate (*SP*/*SP*) background [Ailsa Craig (AC) and Gardener (GRD)], hereafter called *j*(AC) and *j*(GRD), and two in a determinate (*sp*/*sp*) background [Fireball (FB) and Heinz (Hz)], hereafter called *j*(FB) and *j*(Hz).

All *j* mutants lacked flower pedicel AZ, confirming the robustness of this jointless phenotype. By contrast, their inflorescences showed various phenotypes in terms of return to leaf initiation and architecture (**Fig. 1**). In all wild-type (*J*/*J*) backgrounds, >90% of the inflorescences showed the typical monochasial cymoid pattern, with most often 5–8 well-developed flowers, while return to leaf initiation was observed in maximum 10% of them. The different *j* mutants showed a diversity of inflorescence phenotypes that we classified into four categories (**Fig. 1I**): infinite and made of flowers only (IF), as in non-mutated plants; infinite and leafy (IL), made of alternating flowers and leaves; finite and terminated by a leaf (FL); and finite and reduced to a few flowers (FF). The frequency of inflorescences containing leaves (IL and FL types) was >50% in all *j* mutants (**Fig. 1J**). The inflorescences of IL type were very complex since their leaves hosted axillary buds whose outgrowth generated vegetative branches. The observed inflorescence phenotypes barely changed when plants were cultivated at high light intensity (**Supplementary Fig. S1**).

We characterized the inflorescences in more detail and observed that, in the IL type of inflorescences, the number of leaves was higher in *j*(AC) and *j*(GRD) mutants, i.e. in the indeterminate (*SP*/*SP*) genetic backgrounds, than in *j*(FB) and *j*(Hz)mutants, i.e. in the determinate (*sp*/*sp*) ones (**Fig. 1A–H**). Curiously, *j*(Hz) mutant displayed a very regular alternation of one leaf and one flower in IL inflorescences after their return to vegetative growth (**Fig. 1H**). In *j*(FB) mutant, single leaves

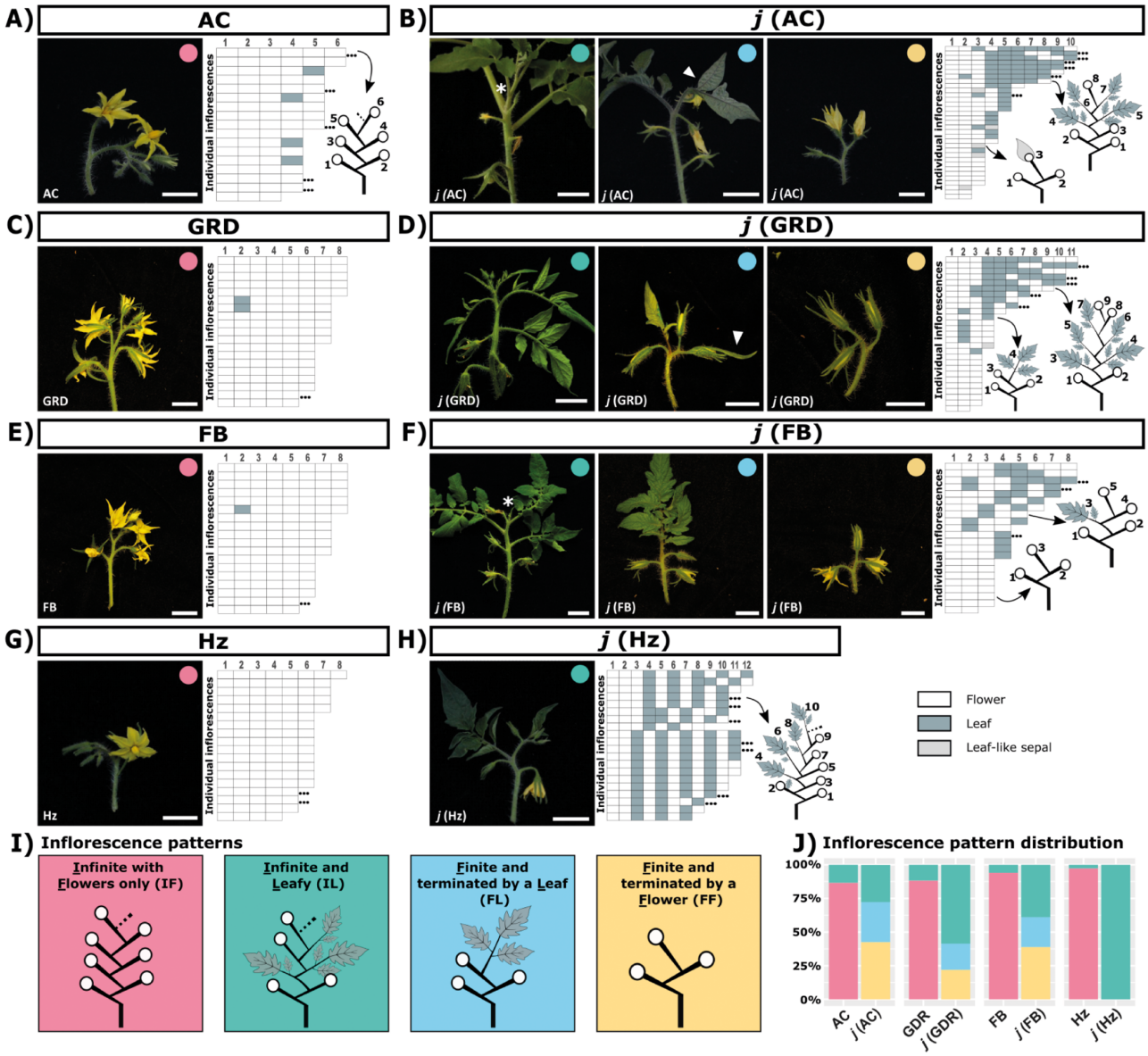

Fig. 1 Inflorescence phenotype of *j* mutants in different genetic backgrounds. Inflorescences of WT and *j* mutants in (A and B) AC, (C and D) GRD, (E and F) FB and (G–H) Hz accessions. Scale bars = 1 cm. On the right side of the images showing representative inflorescences, the composition of >15 inflorescences in each genotype is shown. Each line represents a single inflorescence, and each box represents a flower, a leaf or a flower with an enlarged leaf-like sepal. *X*-axis shows the position along the proximal–distal axis of the inflorescences; *Y*-axis is the stacking of inflorescences that were characterized. Black dots indicate that flower initiation was not finished. White arrowheads show leaf-like sepals, and the asterisk shows an axillary bud at the axil of an inflorescence leaf. (**i**) Inflorescence phenotypes, classified in four patterns: infinite and made of flowers only (IF), infinite and leafy (IL), finite and terminated by a leaf (FL), and finite and reduced to a few flowers (FF). The same colors are used as dots in (A–H) to show the category to which the inflorescences shown belong. The results shown in (J) are from two independent experiments with 20 plants of each genotype. All plants were in the same growth chamber in 16-h long days 150 $\mu E/m^2/s$ light.

also alternated with flowers in the IL inflorescences, but small inflorescences of FF type were more frequent (**Fig. 1F, J**).

In addition to their floral phenotypes, all *j* mutants showed a slight delay of flowering, with the initial shoot segment forming one or two more leaves before the first inflorescence, as compared to their respective non-mutated backgrounds (**Fig. 2B**). Mutant plants were also taller (**Fig. 2C**), and this difference in size was already visible before flowering (**Supplementary Fig. S2**). By contrast, there was little difference in the size of the sympodial segments, which contained one more leaf in *j*(FB) only (**Fig. 2D**). Interestingly, we noticed alteration in shoot branching, more precisely in the timing of lateral bud outgrowth in the different *j* mutants. Precocious axillary development, especially at the first two nodes of the initial segment, was observed

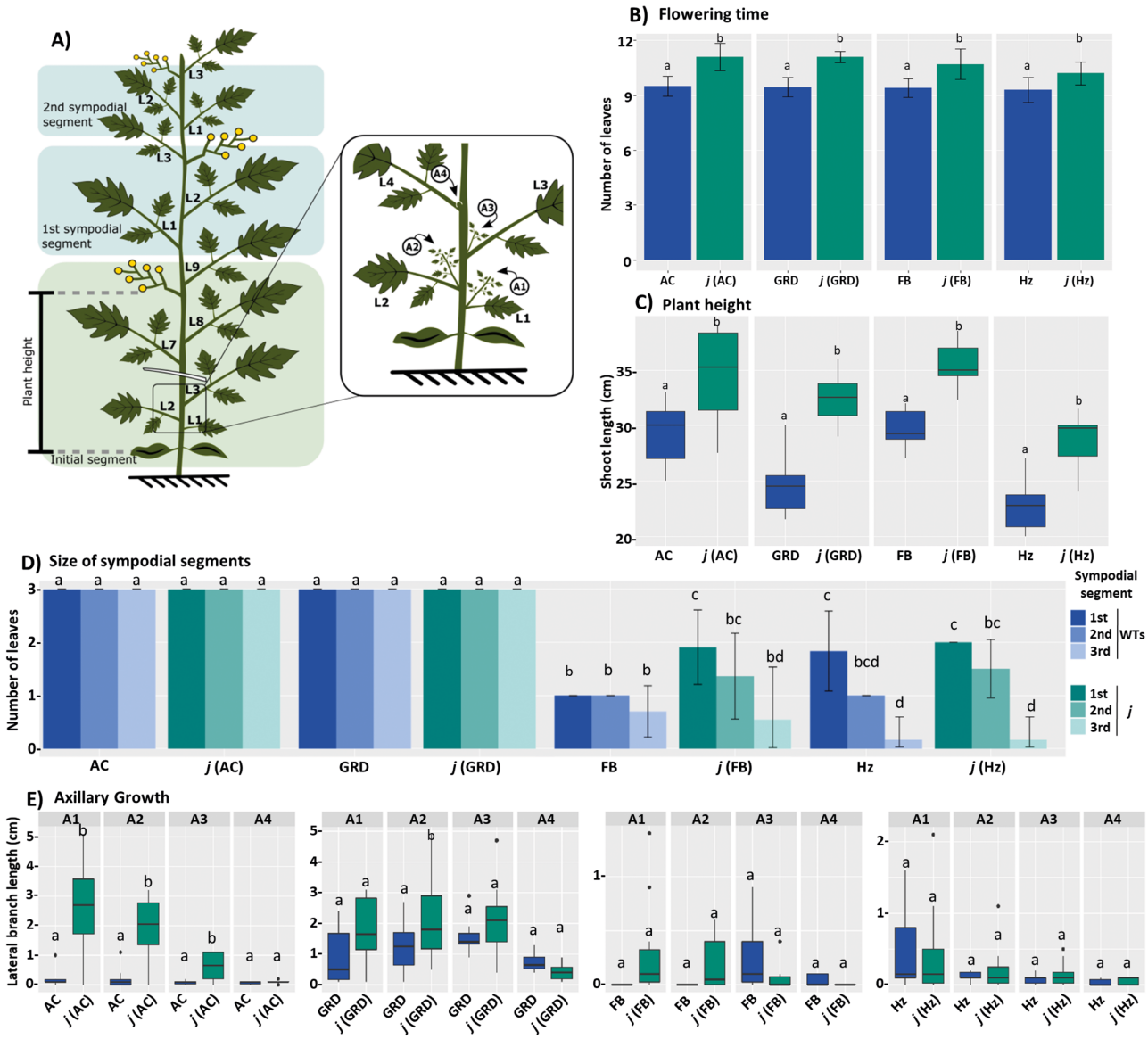

Fig. 2 Shoot phenotype of *j* mutants in different genetic backgrounds. (A) Schematic representation of the shoot traits that were measured. Leaves and axillary branches are numbered acropetally. L, leaf; A, axillary branch. (B) Flowering time measured as the number of leaves below the first inflorescence in WT and *j* mutants in AC, GRD, FB and Hz accessions. (C) Plant height measured at anthesis of the first inflorescence. (D) Number of leaves per sympodial segment. (E) Size of axillary branches in 5-week-old plants. A1–4 designate axillary branches at nodes 1–4 (A). All measurements were done on 10 individual plants per genotype. Results shown are from a representative experiment; similar results were obtained in three independent experiments. Error bars represent the standard deviation; means with different letters are statistically different (Tukey's test, $P < 0.05$).

in *j* mutants but only in indeterminate backgrounds (AC and GRD) and not in the *sp*/*sp* determinate backgrounds (FB and Hz) (**Fig. 2E**).

Transcriptomic analysis of young inflorescence meristems

Transcriptomic analyses were performed in *j* mutants in order to identify regulatory mechanisms of inflorescence development that could explain their phenotypes. We reasoned that harvesting the last two meristems of the inflorescences (**Supplementary Fig. S3**) would avoid inaccurate isolation of single ones and, at the same time, allow capturing the rate of development of the inflorescence, which would be reflected by the relative homogeneity/synchrony of the two successive meristems. Indeed, in wild type (WT) inflorescences, these two meristems are expected to be FM and SIM, and hence, an acceleration of SIM maturation toward FM fate would be reflected by an enrichment in FM markers and increased homogeneity, whereas a deceleration of SIM maturation or its reversion to

vegetative functioning would be correlated with an increased heterogeneity in the meristem transcriptomic profiles. Based on the phenotyping data of *j* mutants (**Fig. 1**), the meristems were harvested from plants dissected shortly after the transition to flowering, in inflorescences that were putatively deviating from the WT pattern after the initiation of 1–3 normal flowers.

Analyses were performed in *j*(AC) and *j*(Hz) mutants in order to capture differences that might be the result of the genetic background and interactions between *J* and *SP*. At first glance, we observed that *j*(Hz) meristems exhibited very few (8) differentially expressed genes (DEGs; $\log_2$Fold Change > 0.5 or <−0.5 and $P_{adj} < 0.05$) as compared to Hz, while the comparison of *j*(AC) and AC meristems revealed a much larger number (565) of DEGs (**Supplementary Fig. S3** and **Supplementary Material, S1**). We also found that AC and Hz accessions differed in the differential expression of 270 genes in their inflorescence meristems, although they do not exhibit macroscopically distinct inflorescences. Since the *j*(AC) mutant had been obtained by a cross between *j*(Hz) and AC plants, we also compared *j*(AC) to Hz and produced an AC×Hz hybrid to check the differential expression of interesting DEGs. We focused the following analyses on three groups of DEGs: eight DEGs between *j*(Hz) and Hz, 22 DEGs between *j*(AC) and both AC and Hz and 376 DEGs between *j*(AC) and AC that were not differentially expressed between Hz and AC (**Supplementary Fig. S3**). We performed a manual sorting of these lists and classified annotated DEGs into functional and homology groups, based on their putative roles in inflorescence development: 'Flowering and Transcription factors', 'Branching and Leaf Growth', 'Hormone and Sugar Signaling' and 'Small RNA Machinery and Chromatin Remodeling' (**Fig. 3** and **Supplementary Fig. S4**).

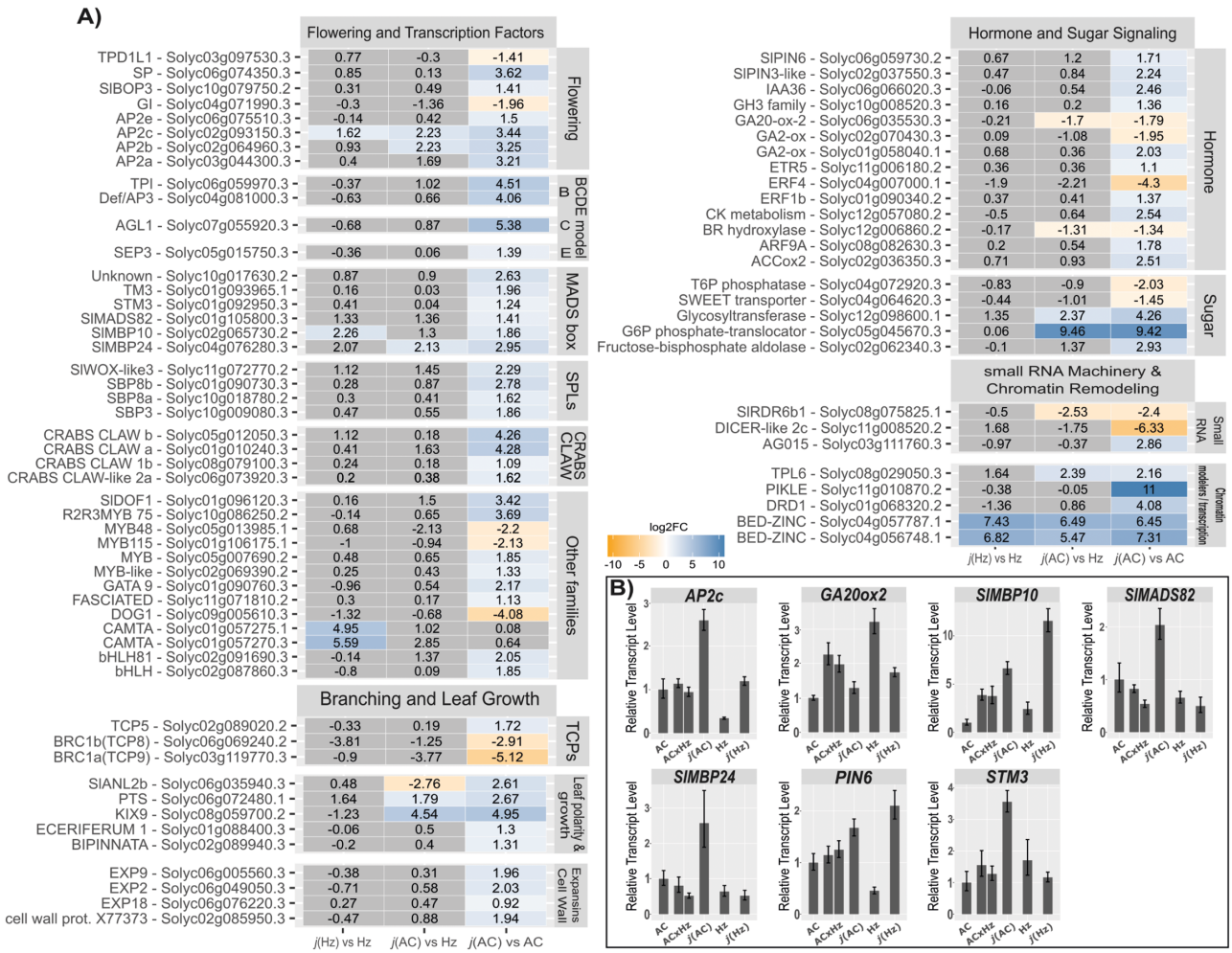

Fig. 3 Transcriptomic analysis of inflorescence meristems in *j* mutants. (A) HeatMap showing the RNA-seq results for DEGs curated manually according to their annotations and their functional classification. Numbers and colors represent the $\log_2$FC in *j* mutants compared to AC and Hz backgrounds. Pairwise comparisons were *j*(Hz) vs Hz (left column), *j*(AC) vs Hz (middle column) and *j*(AC) vs AC (right column). Gray shows non-significant differences, while orange-blue color chart shows DEGs with $\log_2$FC > 0.5 (blue) or <−0.5 (orange) and a $P_{adj} < 0.05$. (B) RT-qPCR validation of differential expression of seven DEGs in independent biological replicates. As a validation of the RNA-seq, only one pool of meristems was harvested for each genotype except for the AC×Hz (*SP*/*SP*) hybrid where two samples (pools of F2 plants) were harvested since it was not included in the RNA-seq analysis. Error bars represent standard deviation on technical replicates.

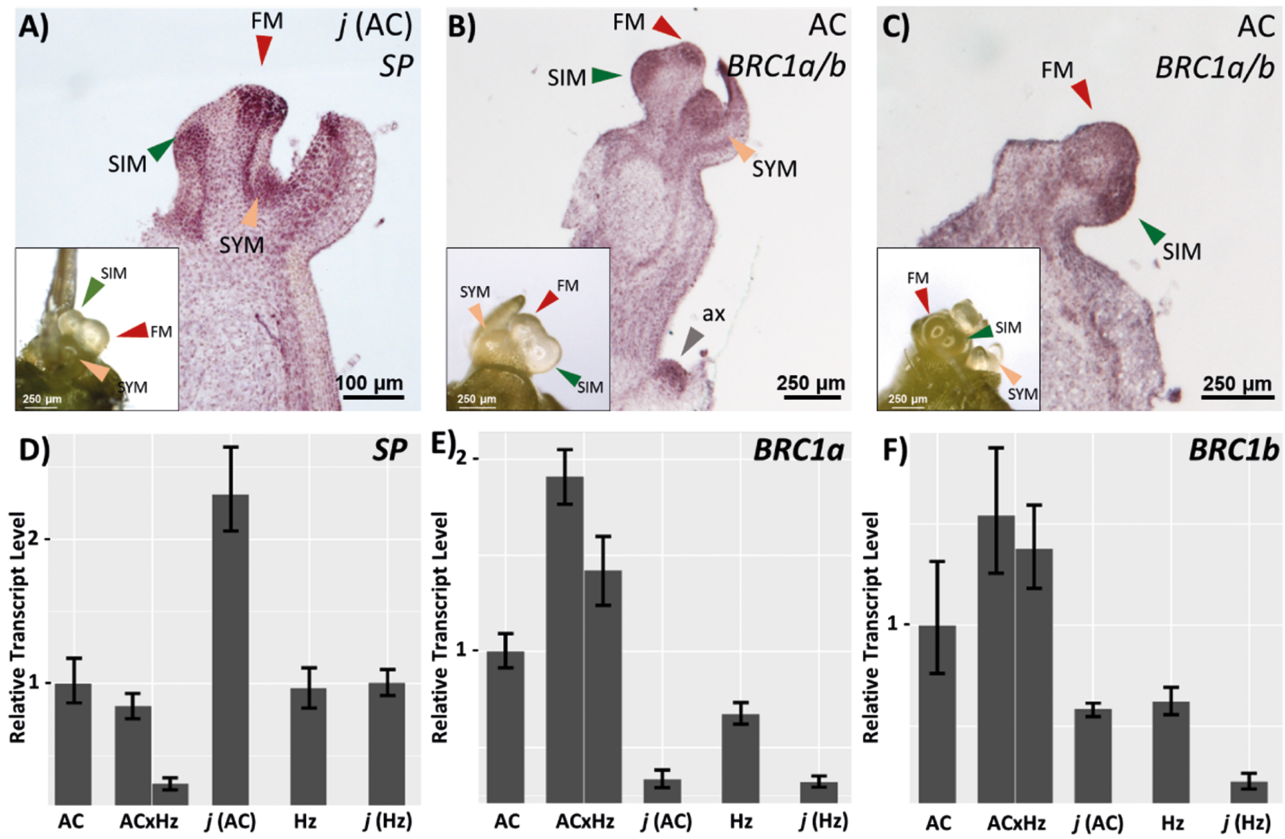

Fig. 4 Expression of *SP* and *BRC1 a/b* genes in AC and *j*(AC) mutant meristems. (A) In situ hybridization using the antisense *SP* probe on longitudinal sections of *j*(AC) obtained from the shoot apex shown in the inset and containing a FM, a SIM and a SYM. (B and C) In situ hybridization using antisense *BRC1a/b* probes on longitudinal sections of AC obtained from the shoot apices shown in insets and annotated as in (A). RT-qPCR validation of differential expression of *SP* (D), *BRC1a* (E) and *BRC1b* (F) in independent biological replicates. As a validation of the RNA-seq analysis, only one pool of meristems was harvested for each *j* mutant, AC and Hz accessions, whereas two samples were harvested for the AC×Hz (*SP*/*SP*) hybrid since it was not included in the RNA-seq analysis. Error bars represent standard deviation on technical replicates.

The reverted inflorescence meristem of j mutants has shoot sympodial fate A major highlight of the transcriptomic analysis was the very low number of DEGs between *j*(Hz) and Hz meristems. This result indicated that the SIM of the *j*(Hz) mutant, although producing one leaf (**Fig. 1H**), transitioned very fast to flowering and did not differ much from the SIM of WT plants. By contrast, in the *j*(AC) mutant, reverted SIM produced more leaves. Moreover, we observed in our RNA-seq analysis, and checked by RT-qPCR, that the *SP* gene was upregulated in the meristems of *j*(AC) mutant compared to AC and AC×Hz plants (**Figs. 3A** and **4D** and **Supplementary Fig. S4**). While we previously showed that *SP* is not expressed in the inflorescence of AC plants (Thouet et al. 2008), we observed by in situ hybridization that *SP* transcripts were detected in both the SIM and FM of *j*(AC) mutant, as well as in the SYM and vasculature (**Fig. 4A**). These results clearly indicate that the reverted SIM of *j*(AC) mutant has adopted a SYM identity.

Flowering genes Among the eight DEGs that were identified in *j*(Hz) vs Hz comparison, we found *APETALA2c* (*AP2c*) and *MADS-BOX PROTEIN 10* (*MBP10*), both of which were upregulated in the mutant (**Fig. 3A, B**). *AP2c* is a member of the *euAP2* clade, a subgroup of the large *AP2/ETHYLENE RESPONSIVE ELEMENT BINDING FACTOR* transcription factor family that is characterized by the presence of two AP2 domains and miR172 recognition site (Kim et al. 2006, Karlova et al. 2011). The *euAP2* clade comprises five members in tomato and owes its name to the *Arabidopsis* gene *AP2*, which was originally identified as an A-class homeotic gene controlling flower organ identity in the perianth. *MBP10* is a MADS-box gene of the angiosperm-specific *AP1/FRUITFULL* (*FUL*) subfamily and more precisely of the *euFULII* clade that contains one additional member in tomato, *MBP20* (Litt and Irish 2003).

The *AP2c* and *MBP10* genes were also upregulated in the *j*(AC) mutant compared to AC or Hz accessions, but more genes were differentially expressed in this background (**Fig. 3A, B** and **Supplementary Fig. S4**). Among them, four of the five *AP2* genes (*AP2a, AP2b, AP2c* and *AP2e*) were upregulated in the *j*(AC) mutant compared to AC. Concerning the MADS-box genes, and based on the molecular and phylogenetic knowledge of this gene family in tomato (Hileman et al. 2006,

Leseberg et al. 2008, Zhang et al. 2018; Wang et al. 2019b, Boumlik et al. 2021), the transcriptomic analysis revealed increased expression in *j*(AC) of the homeotic B-class genes *APETALA3* (*TAP3*, syn. *SlDEF*, *LeAP3*) and *PISTILLATA* (*TPI*, syn. *SlGLO2*) of the C-class gene *AGAMOUS-LIKE 1* (*SlAGL1*) and of the E-class gene *SEPALLATA3* (*SEP3*, syn. *TM5*). Differential expression was also observed for two MADS-box genes of the *SUPPRESSOR OF OVEREXPRESSION of CONSTANS1* (*SOC1*) clade, *TM3* and *SISTER of TM3* and two members of the *SVP*/*AGL24* clade, *SlMADS82* and *SlMBP24*, which were all upregulated in the *j*(AC) mutant (**Fig. 3A** and **Supplementary Fig. S4**).

Another category of genes that were upregulated in *j*(AC) was the *CRABS-CLAW* (*CRC*) subfamily of genes, which belong to the YABBY protein family and are involved in carpel development and FM termination (Gross et al. 2018). Two members, *CRCa* and *CRCb*, showed the largest variation as compared to AC meristems (**Fig. 3A** and **Supplementary Fig. S4**).

Leaf growth and branching genes Since the inflorescences of *j* mutants revert to leaf initiation, one could expect markers of vegetative tissues in the transcriptome of the *j* meristems, providing that a significant proportion of the harvested samples were at the reversion stage. This was indeed the case since genes regulating leaf growth (e.g. *KINASE-INDUCIBLE DOMAIN INTERACTING9, KIX9*), leaf complexity (e.g. *PETROSELINUM* and *BIPINNATA)*, wax biosynthesis (e.g. *ECERIFERUM1*, *CER1*) or cell expansion (e.g. expansins or cell wall proteins) were differentially expressed in the *j*(AC) mutant (**Fig. 3A** and **Supplementary Fig. S4**).

Transcriptomic analysis also revealed that branching genes *BRANCHED1a* (*BRC1a*) and *BRC1b* were downregulated in the meristems of *j*(AC) mutant as compared with the AC genotype (**Fig. 3A** and **Supplementary Fig. S4**). *BRC1* genes are members of the *TEOSINTE BRANCHED1/CYCLOIDEA/PROLIFERATING CELL NUCLEAR ANTIGEN FACTOR1* (*TCP*) family of transcription factors and act as local repressors of lateral bud outgrowth (Wang et al. 2019a). When we checked this result by RT-qPCR, we noticed that the differential expression of *BRC1a* and *BRC1b* between *j*(AC) and AC was mostly due to the fact that the amount of transcripts was higher in AC compared to other genotypes (**Fig. 4E, F**). We therefore performed in situ hybridization on AC meristem sections and observed that *BRC1a/b* was expressed in axillary meristems (including the SYM) and in the inflorescence, where the transcript level seemed higher in the SIM than in the FM (**Fig. 4B, C**).

Sugar and hormone signaling Since *BRC1* genes and lateral bud outgrowth are regulated by multiple hormonal and nutritional signals (Wang et al. 2019a), we scanned the list of DEGs in *j*(AC) mutant in order to identify genes that could indicate modifications in these compounds. An activation of auxin signaling in *j*(AC) meristems could be inferred from higher expression of PIN transporters (*SlPIN6* and *SlPIN3-like*), auxin-regulated genes (*IAA36, GH3-protein*) and auxin response factor (*ARF9a*) (**Fig. 3A, B** and **Supplementary Fig. S4**). We also identified one cytokinin metabolism gene that was upregulated in the meristems of *j*(AC) mutant. The gibberellin content was unpredictable since one biosynthetic GA20-oxidase was downregulated, while two inactivating GA2-oxidases showed opposite changes.

Concerning sugar metabolism, we observed strong upregulation of a *GLUCOSE-6-PHOSPHATE-TRANSLOCATOR* gene in *j*(AC) meristems, downregulation of a sucrose exporter (*SWEET*) and downregulation of *TREHALOSE-6-PHOSPHATE PHOSPHATASE* (*TPP*) gene whose product dephosphorylates Trehalose-6-P (Tre6P) (**Fig. 3A** and **Supplementary Fig. S4**). These modifications, especially the downregulation of *TPP*, might indicate an increase in sugar and Tre6P content in the meristems of *j*(AC) mutant.

Phenotypes of 35S:*J* plants

In order to further analyze the role of the *J* gene, overexpressing lines were produced. More than 20 independent *35S:J*(AC) lines were obtained and showed a robust phenotype. The inflorescences of these transgenics were made of flowers with much enlarged, leaf-like and partially fused sepals enclosing underdeveloped petals, stamens and carpels (**Fig. 5A, B**).

The arrested growth of reproductive organs in *35S:J* (AC) flowers caused sterility, and hence, T0 plants had to be propagated vegetatively. Only three T0 plants, after several months of growth, formed small fruits, and we could obtain one homozygous T2 line whose flowering time was slightly delayed (about one more leaf than in AC control plants), although the difference was not statistically significant (**Fig. 5C**). The phenotype of the flowers was identical to that observed in T0 plants.

In addition to the extreme calyx phenotype, the flowers of *35S:J* (AC) plants showed elongated pedicels with no or abnormal AZ (**Fig. 5A, B**). Amazingly, when an abnormal AZ was noticed, it was misplaced at the base of the calyx and the internode between the calyx whorl and the inner organs of the flower was elongated (**Fig. 5E**). Histological sections confirmed the presence of a dense set of cells in the internal tissues of the pedicel where the abnormal AZ was formed, but unlike what was observed in normal pedicels of AC flowers, this zone did not expand radially toward the external tissue and epidermis of the pedicel (**Fig. 5D, E**). We harvested this 'pseudo AZ' in independent *35S:J* (AC) T0 plants in order to analyze the expression of AZ marker genes *Bl*, *Ls*, *SlWUS* and *GOB* in comparison with normal AZ of AC plants and jointless pedicel of *j*(AC) mutant (**Fig. 5F**). The results showed a large variability among the *35S:J*(AC) plants, although all of them showed high expression of *J* in the harvested tissues. One transformant (#4) showed increased expression of the four AZ marker genes in the 'pseudo AZ', but the activation of *SlWUS* was much less than that in normal AZ of the AC flower (**Fig. 5F**). In the other *35S:J*(AC) plants, *Bl* and *GOB* genes were activated at a lower or at a most similar level than in normal AZ of AC flowers, whereas *Ls* and *SlWUS* were not activated. These results suggest that the 'pseudo AZ' is indeed an abnormal AZ with an incomplete transcriptomic signature.

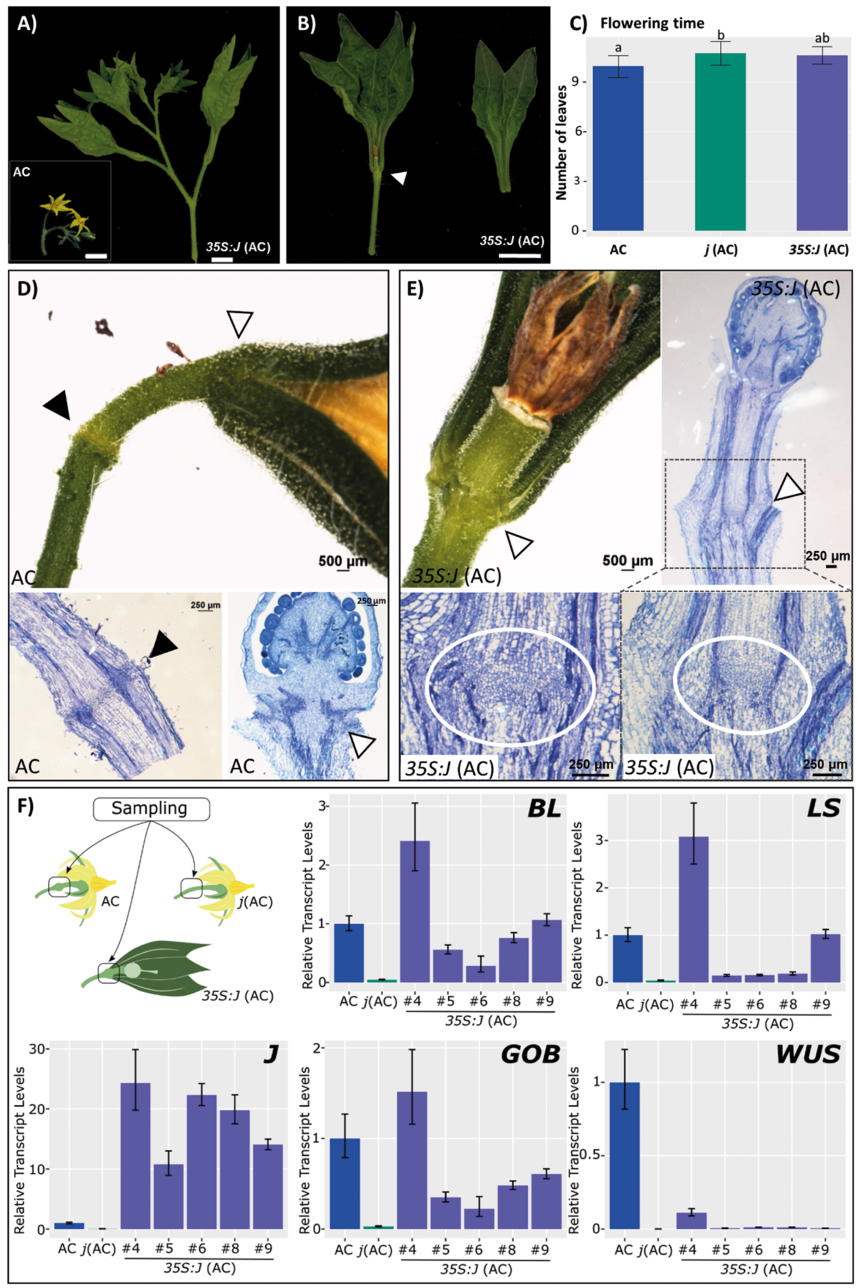

Fig. 5 Phenotypes of *35S:J* plants in an indeterminate AC background. (A and B) Inflorescences of two representative independent *35S:J* (AC) T0 plants, showing elongated leaf-like sepals fused at their base, elongated pedicel and lack of AZ, compared to AC [inset in (**A**)]. In (B), sepals were detached to show the inner whorls. White bar scales in (A) and (B) = 1 cm. (**C**) Flowering time of one homozygous *35S:J* T2 line, measured as the number of leaves below the first inflorescence; $n = 20$ for AC and *j*(AC); $n = 8$ for the *35S:J* line due to seed limitation. Error bars represent standard deviation. Means with different letters are statistically different (Tukey's test, $P < 0.05$). (D) AC flower pedicel and histological sections of AZ (bottom left) and sepal attachment whorl (bottom right). (E) *35S:J* (AC) flower and histological sections of 'pseudo AZ' at the sepal attachment whorl. The ellipses show the inner set of dense and small cells that are typical of AZ. Black arrowheads point AZ, white arrowheads point sepal attachment whorl. (F) Molecular analysis of *35S:J* (AC) pseudo AZ. Schematic representation of sampling of AC pedicel AZ, *j*(AC) jointless pedicel and *35S:J* (AC) 'pseudo AZ' at the attachment of sepals. RT-qPCR analysis of *J* and AZ genes: *Bl*, *GOB*, *Ls* and *SlWUS*. Error bars represent standard deviation on technical replicates.

Transcriptomic analyses of inflorescence meristems were performed in the *35S:J* (AC) plants using 20 T0 independent lines and the same harvesting protocol as for *j* mutants. Compared to the AC genetic background, 216 DEGs were found (**Supplementary Material, S1**). However, besides housekeeping genes, only a few interesting candidates were iden-

tified (**Supplementary Fig. S5**). Among them, the auxin transporter *SlPIN3* was upregulated in the meristems of the *35S:J* plants. Unexpectedly, other changes were common to *j*(AC) mutant, since we observed in *35S:J*(AC) meristems upregulation of *SP*, *TM3* and *KIX9* and downregulation of *BRC1b*.

Discussion

J represses SYM fate in the inflorescence

The *j* mutant of tomato was first isolated for the lack of flower pedicel AZ (Butler 1936), and this phenotype was observed here in four different genetic backgrounds, supporting that the J protein plays a critical role in the initiation of this breaking point. By contrast, the undesired effect of *j* mutation on inflorescence development and its return to leaf initiation was much more variable. We observed that the number of leaves interpolated between flowers in the inflorescences of *j* mutants was higher in indeterminate (*SP*/*SP*) backgrounds (AC and GRD) than in determinate (*sp*/*sp*) backgrounds (Hz and FB). This result is consistent with the statement that '*sp* mutation masks the leafy inflorescence phenotype and hence is epistatic to *j*' (Rick and Sawant 1955, Rick and Butler 1956), although the leafy phenotype of *j* was not completely suppressed in the *sp*/*sp* accessions used here. These observations indicate that the reversion of the inflorescences in *j* mutants is due to the adoption of SYM fate by the SIM. This was also hypothesized from genetic experiments by Szymkowiak and Irish (2006) who reported that the leafy inflorescence phenotype due to *j* mutation was suppressed in *blind* mutant that does not form SYM. Differential expression of the *Bl* gene was not detected in the transcriptomic analysis performed here, but we found that *SP* is upregulated in the inflorescence of the *j*(AC) mutant, whereas in WT plants, *SP* is not expressed in the inflorescence but in the SYM and other axillary meristems (Thouet et al. 2008). These results are consistent with the loss of SIM identity in *j* mutants and its replacement by a SYM where *SP* is expressed. Moreover, we observed that *j* mutation had little impact on the transcriptional profile of meristems in the Hz (*sp*/*sp*) background. This can be explained by the fact that, even if conversion of the SIM into SYM occurred, its faster transition to FM due to the *sp* mutation has a compensatory effect. Whether *SP* is a direct or indirect target of J and whether the upregulation of *SP* in the SIM is the cause or the consequence of its conversion to SYM in *j* mutants cannot be ascertained from transcriptomic data.

J regulates branching

The sympodial pattern of inflorescence formation in tomato implies that the SIMs are initiated as lateral meristems. It is thus interesting to note that differential expression of genes involved in inflorescence or shoot branching was found in the *j* mutants.

MBP10 is a member of the *eu-FULII* clade of MADS-box transcription factors, which includes *Arabidopsis AGL79* gene (Hileman et al. 2006). It was recently proposed that *MBP10* has lost gene function, since it shows an atypical structure, very low expression level and fast evolution (Maheepala et al. 2019), and the CRISPR-mediated loss of function of *MBP10* does not produce any visible phenotype (Jiang et al. 2022). Although these data do not substantiate the upregulation of *MBP10* in the meristems of *j*(AC) and *j*(Hz) mutants, it is interesting to emphasize that *AGL79-like* genes regulate inflorescence branching in legumes forming compound racemes, by repression of *SP* homologs (Berbel et al. 2012, Cheng et al. 2018). Given the sympodial pattern of the tomato inflorescence, the SIM can be regarded as a secondary inflorescence axis forming a single flower, and hence, the expression of the *AGL79-like* gene *MBP10* can be meaningful.

BRC1 genes are widely conserved across angiosperms and play a key role in regulating shoot branching (Wang et al. 2019a). High expression of *BRC1* is associated with arrested axillary buds, whereas expression decreases upon bud activation. In tomato, two *BRC1* paralogs were identified, *SlBRC1a* and *SlBRC1b*, but only *BRC1b* seems to have conserved the ancestral function (Martin-Trillo et al. 2011). Although both genes were reported to be expressed in floral organs, no inflorescence phenotype was observed in *BRC1a* neither *BRC1b* RNAi lines (Martin-Trillo et al. 2011). Since the expected phenotype would be an accelerated outgrowth of the lateral SIM, this might have been unnoticed. We detected by in situ hybridization expression of *BRC1a/b* in the young inflorescence meristems of AC plants, and the RNA-seq analyses indicated their downregulation in the *j*(AC) mutant. These results suggest that transient expression of *BRC1a/b* genes in the inflorescence of tomato might delay lateral SIM outgrowth and that this is somehow regulated by *J*. Interestingly and consistent with this hypothesis, we observed increased shoot branching in *j*(AC) mutant and Thouet (2011) previously observed that *J* is expressed in axillary meristems (**Supplementary Fig. S6**). It is well documented in the literature that shoot lateral bud outgrowth responds to physiological signals (Barbier et al. 2019). It is then interesting that some of these signaling pathways showed differential expression in the inflorescences of *j*(AC) mutant, especially Tre6P that is important for inflorescence branching in maize (Satoh-Nagasawa et al. 2006).

Altogether, the RNA-seq study of *j*(AC) mutant suggested an acceleration of lateral bud outgrowth in the inflorescence, as indicated by downregulation of *BRC1* genes and upregulation of the putative secondary inflorescence meristem *AGL79-like* (*MBP10*) gene. The outgrowing lateral meristem in the inflorescence is ontogenetically the SIM, which can switch to SYM fate in *j* mutants. One biological function of *J* in WT inflorescence would thus be to refrain lateral SIM outgrowth, possibly by interfering with the *BRC1* hub.

J regulates SIM fate

Inflorescence meristems have an intermediate fate, which requires that both the return to vegetative functioning and the premature maturation to FM fate must be refrained.

The return to vegetative functioning in the inflorescences of *j* mutants is correlated with the conversion of the SIM into

a SYM that undergoes a short vegetative phase (see earlier). The fact that *j*(AC) and *j*(Hz) meristems are in a more vegetative stage is also reflected by the higher expression of *AP2-like* genes that was detected in the RNA-seq experiment. It is known indeed that, beyond floral organ identity, *AP2*-like genes act as repressors of floral transition (Yant et al. 2010). The tomato genome contains a family of five *AP2* genes, whose distinct expression patterns indicate different functions (Karlova et al. 2011). Based on single-meristem transcriptomic analyses, Meir et al. (2021) showed that the expression of *AP2c* is associated with the vegetative phase and decreases after the transition to flowering. Importantly, we observed upregulation of *AP2c* in both *j*(AC) and *j*(Hz) mutants. We cross-examined our list of DEG with the 288 stage-related feature genes identified by Meir et al. (2021) and found 30 common genes (**Supplementary Table S1**). Eleven of them—including *AP2c*—were part of the 'vegetative' signature of pre-transition meristems, and 15 of them were found to be activated at late-transition or flower initiation stages. This latter class includes *SEP3*, which we found to be upregulated in *j*(AC) mutant.

Besides the return to leaf initiation, *j* mutants exhibited another inflorescence phenotype: some inflorescences stopped after the initiation of only two or three flowers (**Fig. 1**). The number of flowers in the tomato inflorescence is explained by the rate of meristem maturation (Lippman et al. 2008), a reduced number of flowers resulting from accelerated development. Consistently, we observed in the *j*(AC) mutant the upregulation of DEGs that are orthologous to genes of the ABCDE model of floral development. The RNA-seq data showed in *j*(AC) mutant upregulation of the B-class genes *TAP3* and *TPI*, which are mainly expressed in petal primordia (de Martino et al. 2006, Quinet et al. 2014), and of the C-class gene *SlAGL1*, also known as *ARLEQUIN* (Gimenez et al. 2016). Together with *SlAG1*, *SlAGL1* performs a homeotic C-function by repressing the A-function in the carpels. Interestingly, *SlAGL1* was suggested to repress *J* because the gain of function *alq* mutant lacks the flower pedicel AZ and shows reduced expression of *J* (Pineda et al. 2010). Since we observed upregulation of *SlAGL1* in *j*(AC) mutant, these data suggest a mutual repression of *SlAGL1* and *J*. The RNA-seq analysis also revealed the upregulation of *CRC* orthologs in *j*(AC) mutant. Two genes of this family, *CRCa* and *CRCb*, which were the most upregulated in *j*(AC) mutant, were recently shown to be involved in FM termination, since loss-of-function CRISPR-edited plants exhibit carpel-inside-carpel phenotype (Castaneda et al. 2022). These results are consistent with an acceleration of meristem maturation in the inflorescences of *j*(AC) mutant. It is worth noting that we did not find differential expression of FM identity genes such as *FA* or *AN*, and hence, the effect of *J* on FM maturation occurs at a later stage than we previously hypothesized (Thouet et al. 2012). It is also worth noting that no transcriptional sign of accelerated meristem maturation was identified in *j*(Hz) mutant that, consistently, also did not exhibit the phenotypic signs of fast inflorescence development (i.e. reduced flower number), in contrast to the other *j* mutants examined in this study. One explanation might be that the Hz accession itself manifests faster meristem maturation as suggested by our data (**Supplementary Fig. S4**) and that the *j* mutation does not cause any further effect in this background.

In summary, the transcriptomic analyses of *j*(Hz) and *j*(AC) mutants suggest the maintenance of a pre-transition state in *j* mutants, indicated by the *AP2c* marker, which in *j*(AC) mutant is superimposed on the activation of homeotic genes of B- and C-classes. The biological function of *J* in the inflorescence of WT plants would thus be to repress the vegetative fate and refrain FM maturation in the SIM. The transcriptomic analysis performed here interestingly provides molecular insights into the dual role of *J* that we previously suggested from a modeling approach of tomato inflorescence ontogeny (Périlleux et al. 2014). This model followed simple rules and was based on two variables: the initial 'vegetativeness' of the meristems being initiated in the inflorescence and their maturation rate toward floral commitment. We tested how these variables had to be adjusted to generate different inflorescence phenotypes as an output of the model, and we found that the phenotype of *j* mutants needed an increase in both the initial vegetativeness and the maturation rate of the meristems. Although this was pure modeling, the RNA-seq data provided here strikingly lead to the same conclusion, thus reinforcing arguments that *J* does indeed repress vegetative fate and influence maturation to floral fate in the SIM.

J and MC share overlapping functions

If the RNA-seq analysis of *j* mutants provided data that were consistent with the phenotypes of the plants, scarce transcriptomic changes were found in *35S:J*(AC) plants and those changes were mostly similar to those described in *j*(AC) mutant, suggesting a dominant negative effect of the overexpression of *J*. Most intriguingly though, *35S:J*(AC) plants, despite the upregulation of *SP* in the meristems, did not return to leaf initiation but formed very large inflorescences made of sterile flowers with leaf-like sepals. The calyx of *35S:J*(AC) plants was not inflated, but its size, fusion and enveloping shape are similar to those of the 'inflated calyx syndrome' (ICS) of some *Solanaceae*, especially *Physalis pruinosa* ('Chinese lantern') where it was best studied. The ICS phenotype of *Physalis* has been explained by the heterotopic expression of a MADS-box gene called *MPF2* (He and Saedler 2005). This was, however, recently re-evaluated in view of the fact that CRISPR-Cas9 targeted loss-of-function mutation of *MPF2* does not suppress calyx inflation per se, i.e. the encapsulation of the fruit by excessively large sepals (He et al. 2023). *MPF2* belongs to the same *AGL24/SVP* clade as *J*, and leafy sepals were obtained by overexpression of *AGL24/SVP* genes in other *Solanaceae*, e.g. in *Petunia* (Li et al. 2016). Interestingly, the *MPF2* gene of *Physalis* is repressed by the MPF3 protein, which is orthologous to MC (Zhao et al. 2013). This could explain that loss of *MC* function causes a 'macrocalyx'

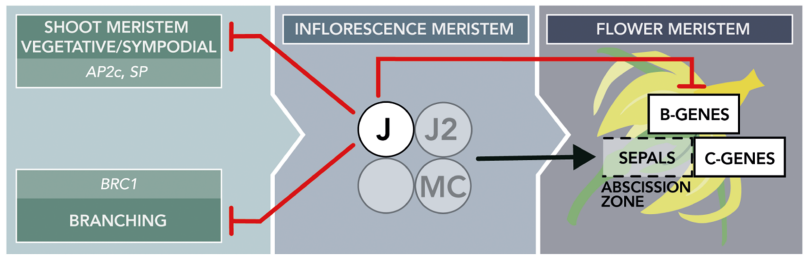

Fig. 6 Model of *J* function in the inflorescence meristem of tomato. J plays a pivotal role in the inflorescence meristems of tomato, by repressing shoot sympodial meristem fate and return to vegetative functioning, and by influencing reproductive flower organ formation. This was shown by differential expression of marker genes such as *SP, AP2c* and homeotic genes of B- and C-classes in *j* mutant, in an indeterminate (AC) background. These functions of *J* might start upon the initiation of the inflorescence meristems since differential expression of branching genes such as *BRC1* was also found. It is not known whether J plays these roles in the same MADS-box protein complex (shaded) that includes J-2 and MC and is thought to regulate the concomitant initiation of sepals and pedicel AZ. It is not known either whether the effects of J on the genes included in this model are direct or indirect. A-class genes are not shown since no gene whose mutation causes homeotic conversion of sepals is known in tomato.

phenotype, although this was generally justified by the orthology of *MC* to the A-class gene *AP1* of *Arabidopsis* (Vrebalov et al. 2002, Yuste-Lisbona et al. 2016). Differential expression of *MC* did not appear in our transcriptomic analyses of *j* mutants or *35S:J* plants. However, since J and MC proteins physically interact (Nakano et al. 2012), phenotypes can be due to the fact that MADS-box complexes that include J and MC are not functional when J is not present or is overabundant. As such, the absence of functional J protein in *j* mutants or its overabundance in *35S:J* plants might have the same effect as the absence of MC. Consistently, the *mc* mutants share with *j* other phenotypes: they undergo reversion of the inflorescences to vegetative growth after the initiation of a few flowers and also form abnormal flower pedicel AZ (Yuste-Lisbona et al. 2016). The *mc* and *j* mutations have additive effects: in the double *j mc* mutant, reversion of the inflorescence to leaf initiation occurs after the initiation of only one flower (Yuste-Lisbona et al. 2016), indicating that J and MC together regulate the fate of the inflorescence meristems.

Is the *j* phenotype just pleiotropic ?

All *j* mutants described in this study lacked the 'canonical' flower pedicel AZ. We did not, however, detect DEGs among the genes that are known to be upregulated in AZ, neither in *j*(Hz) nor in *j*(AC) mutants, most probably because the inflorescence meristems were harvested too early with respect to AZ formation. Interestingly, the lack of AZ in the *35S:J* plants is consistent with a dominant negative effect of *J*, as suggested earlier for the identity of sepals. A protein complex comprising J, J2 and MC was indeed postulated to regulate the formation of the AZ, since the lack of any of these MADS-box protein partners abolishes, totally or partially, the formation of the flower pedicel AZ (Liu et al. 2014, Gomez-Roldan et al. 2017). The absence or overabundance of the J protein would thus affect the functionality of this complex and impair AZ formation. We observed, however, in *35S:J*(AC) plants that a pseudo AZ developed but was misplaced at the attachment of leafy sepals, which further supports the idea that the formation of the AZ and the identity of the first whorl of floral organs are intertwined processes sharing regulatory networks (Périlleux and Huerga-Fernández 2022).

The transcriptomic analyses that we performed here in *j* mutants extended the functions of *J* to the early steps of meristem development in the inflorescence and led to the model proposed in **Fig. 6**. *J*, by repressing vegetative/SYM fate and by influencing reproductive flower organs formation, holds the inflorescence meristems in a transient fate during which they maturate toward AZ and sepal initiation. The effects of *J* on branching genes suggest that *J* acts upon the initiation of the lateral SIM and thus bridges branching and development in tomato inflorescence. The next challenge will be to dissect the spatio-temporal network that mediates this transient function of *J*, which is critical for SIM identity.

Materials and Methods

Plant material and growth conditions

Seeds of the *j* mutant in the determinate accession Hz, carrying *sp* mutation, were obtained from the Institut National de la Recherche Agronomique (INRA Montfavet, France) (Philouze 1978). The *j* mutation was introduced by crossing in the indeterminate accession AC carrying the *SP/SP* allele. F2 plants were selected based on the jointless phenotype and the absence of *sp* mutation and were propagated by self-pollination (Quinet et al. 2006, Thouet et al. 2012). As a control, an AC×Hz hybrid was produced by pollinating AC flowers with Hz pollen and genotyping F2 plants for homozygous *SP/SP* alleles. Seeds from AC (LA2838), FB (LA3024), *j*(FB) (LA3023), GRD (LA3030) and *j*(GRD) (LA3033) were obtained from the Tomato Genetics Resource Center. All *j* and *sp* alleles are shared by the different accessions: the *j* mutation is a 939-bp deletion including part of the MADS-box (Mao et al. 2000); the *sp* mutation is a single base substitution (Pnueli et al. 1998). These mutations do not suppress transcription of the genes.

Seeds were sown in jiffy pots for germination in plastic greenhouses. At the 4–5 visible leaf stage, plants were transferred into 2.5-l pots filled with a mixture of compost and perlite (80/20, v/v) and kept in growth chambers in 16-h long days, at 21–23°C, 70–80% relative humidity and 100–150 μmol/m^2 s^1 light (fluorescent tubes). Plants were watered daily with tap water and were fertilized weekly with 'Engrais Universel Bleu Novatec' (COMPO, Münster, Germany).

Phenotypic analyses

Flowering time was measured as the number of leaves below the first inflorescence. The architecture of the inflorescences was characterized in terms of number and position of flowers and leaves.

Growth of the axillary branches was measured for 5-week-old plants. Axillary branches were isolated from the main shoot with a scalpel and measured from their base up to their apical bud.

Genotyping

DNA was extracted using the CTAB method from fresh or snap-frozen plant material (stored at −80°C). PCR amplifications were performed in 20 µl of reaction mixtures containing 50–100 ng of DNA, 0.25 mM dNTP mix (Promega Corp., Madison, Wisconsin, USA), 0.25 µM primers (Integrated DNA Technologies, Coralville, Iowa,USA) (**Supplementary Table S2**), 1 U/µl DNA polymerase and 1× DNA polymerase buffer in nuclease-free water (Ambion®). Two types of polymerase were used: Phusion II Hot Start polymerase (ThermoFisher Scientific Inc., Waltham, Massachusetts, USA) for sequence cloning and GoTaq (Promega Corp., Madison, Wisconsin, USA) for other purposes.

Transcriptomic analyses

RNA extraction *RNA* extraction was performed from snap-frozen plant material (stored at −80°C) with the NucleoSpin *RNA* Plant® kit (Macherey-Nagel, Duren, Germany), following the manufacturer's instructions. Purified RNA was eluted in 40 µl of nuclease-free water (Ambion®). The absence of genomic DNA contamination was checked by PCR-amplifying a genomic sequence of the tomato *UBIQUITINE* gene (*UBQ*, Solyc01g056940) (primers in **Supplementary Table S2**).

qPCR analyses A total of 1 µg of extracted RNA was used for synthesizing cDNA in 20 µl of reaction mix of 6.5 U/µl MMLV Reverse Transcriptase (Promega Corp., Madison, Wisconsin, USA), 25 ng/µl oligo$(dT)_{15}$ and 400 µM dNTPs. The tubes were placed for 10 min at 40°C, 90 min at 55°C and 15 min at 70°C. Thereafter, samples were diluted in 70 µl of nuclease-free water and stored at −20°C until use. qPCR was performed in technical triplicates in 384-well plates, using a QuantStudio 5 thermocycler (Applied BioSystems, ThermoFisher Scientific Inc., Waltham, Massachusetts, USA). Reactions were performed in a final volume of 10 µl [2 µl of cDNA, 5 µl of Takyon™ Low ROX SYBR® Mastermix dTTP Blue (Kaneka Eurogentec S.A., Seraing, Belgium), 0.25 µl of each 10 µM primer (primers in **Supplementary Table S2**) and 2.5 µl of H_2O]. The qPCR standard run program consisted of a hold phase (2 min. at 50°C and 10 min. at 95°C) followed by 40 cycles (15 s at 95°C, 1 min. at 60°C). C_q values and comparative cycle threshold (ΔΔCT) were analyzed using QuantumStudio DA2 (ThermoFisherApp), with *UBQ* as housekeeping reference gene for data normalization.

RNA-seq analysis Transcriptomic analyses by RNA-seq were performed on four biological replicates per genotype. Each replicate (sample) was a pool of 60–90 pairs of meristems, consisting of the two youngest meristems of an inflorescence. The independent replicates were obtained from independent plant cultivations, which were all done under the same growth room and environmental conditions. All dissections were performed between 9:00 a.m. and 11:00 a.m. under a stereoscopic microscope, using scalpels and glass supports that were previously cleaned with RNase AWAY (Molecular bioProducts, Toronto, Canada). The meristems were immediately fixed in ice-cooled acetone (96% purity) and stored (maximum 2 d) at −80°C until extraction. Fixed meristems were ground and homogenized with a Ball Mixer Mill (MM200, Retsch GmbH, Haan, Germany), and RNA extraction was performed as described earlier. A total of 1 µg of RNA in a final volume of 50 µl was required per sample. RNA sequencing was performed using GIGA-Genomics Platform (ULiège, Belgium; https://www.gigagenomics.uliege.be) after a quality control. The TruSeq Stranded mRNA Library Prep Kit (Illumina, San Diego, California, USA) and a NovaSeq (Illumina) sequencing system were used. At least 20 10^6 reads were obtained for each sample.

The read quality of the samples was analyzed using the FASTQC bioinformatic tool (www.bioinformatics.babraham.ac.uk/projects/fastqc/). For some samples, due to the sequencing method, over-represented guanine tails (polyG) were found and were removed using prinseq software (http://prinseq.sourceforge.net/manual.html#DP). The quality trimming and the removal of adapters were performed using TRIMMOMATIC (Bolger et al. 2014). After trimming, mapping of the reads was conducted using TopHat (http://ccb.jhu.edu/software/tophat) and ITAG3.2 version of tomato genome (www.solgenomics.net). Mapped reads were counted with the htseq-count tool (Anders et al. 2015), and a read count/gene matrix was generated. Finally, the gene count matrix was used to identify the statistically DEGs in pairwise comparisons of the samples performed with *R* package DESeq2(Love et al. 2014). Specifying the minimum effect size (lfcThreshold = 0.5), genes were considered as DEGs when $|Log_2FoldChange|$ was >0.5 and the adjusted *P*-value after false discovery rate was <0.05. Normalized read count graphs were generated using the plotCounts option of the DESeq2 package.

Transgenic plants generation

Vector construction The open reading frame of the *J* gene (*Solyc11g010570*) flanked with the recombination sites attB1 and attB2 was synthesized by PCR (primers in **Supplementary Table S2**), using cDNA from young inflorescences of tomato (AC accession) as a template. These sequences were cloned into pDONR221 vector (addgene.org) by a BP Gateway ® (Invitrogen, ThermoFisher Scientific Inc., Waltham, Massachusetts, USA) reaction. The overexpression vector was generated with a LR reaction Gateway® (Invitrogen) with a binary vector pK7WG2.0 (addgene.org; Addgene, Watertown, Massachusetts, USA) that contains a CaMV35S promoter and terminator in the backbone, along with a kanamycin resistance gene. The *35S:J* vector was used to transform thermo-competent *Agrobacterium tumefaciens* strain GV3101-pMP90 by heat shock.

Transformation of tomato Tomato seeds were sterilized in 2.7% sodium hypochlorite (half-strength standard bleach) for 10–25 min. They were rinsed with sterile water several times, then sown in sterile jars containing germination medium [0.22% Basal MS (Duchefa, Haarlem, The Netherlands), 1.5% saccharose, 0.8% Agar (Kalys, Bernin, France)]. When fully expanded, cotyledons were cut and placed for 24 h on pre-culture medium [0.44% MS including vitamins (Duchefa), 2.5% saccharose, 0.8% agar, $1/10^7$ IAA w/v (Sigma-Aldrich, Merck KGaA, Darmstadt, Germany), $2/10^7$ BAP w/v (Sigma-Aldrich, Merck KGaA, Darmstadt, Germany)] under diffuse light. Thereafter, they were incubated for 20 min in a liquid culture of *A. tumefaciens* cells in MS, 3% saccharose and 0.2 mM acetosyringone (Sigma-Aldrich, Merck KGaA, Darmstadt, Germany) at an optical density of 0.4–0.6 (600 nm). After the incubation, the explants were dabbed with sterile paper and transferred onto a co-culture medium (pre-culture medium including 0.2 mM acetosyringone) for 48 h under diffuse light. To eliminate excess of bacteria, the explants were washed at least 4 times with 0.5% Tween20 (v/v), dried on sterile filter paper and placed on regeneration medium [same as pre-culture medium, with additional 0.03% Timentin (Duchefa, Haarlem, The Netherlands) and 0.015% kanamycin w/v (Sigma-Aldrich, Merck KGaA, Darmstadt, Germany) for selection] in Petri dishes sealed with parafilm and placed under light. Explants were transferred on fresh regeneration medium every 2 weeks. Emerging shoots were isolated and transferred onto rooting medium (same as germination medium, with additional 0.03% Timentin and 0.015% kanamycin).

Transgenic plant isolation and propagation Rooted shoots were acclimated in soil-containing jiffy pots, in small plastic greenhouses, and were genotyped for the presence of the 35S promoter (primers in **Supplementary Table S2**). Fruits of these T0 plants were harvested, and T1 seeds were sown; T1 plants showing a similar phenotype than T0 plants were selected and used

for T2 seed harvest. T2 seeds were sown in vitro on germination medium containing 0.015% kanamycin to select lines showing 3:1 resistance segregation (suggesting a single T-DNA insertion). The resistant T2 plants were used to produce T3 seeds, and those showing 100% resistant T3 progeny were selected as T2 homozygous lines.

Due to the sterility problem of most *35S:J* T0 plants in the AC background, they were propagated by cuttings of lateral shoots. Cuttings were dipped in 0.05% nutrient solution Flora Series GEH v/v (General Hydroponics, Santa Rosa, California, USA) until rooting and then transplanted in soil-containing 2.5-l pots as described in the Plant material and growth conditions section.

Histological sections

Young inflorescences and flower pedicels were dissected under the binocular stereoscope and fixed in FAA (50% ethanol, 10% 37%-formaldehyde, 5% acetic acid) at 4°C overnight. After paraffin embedding, sections of 5–8 μm were made with a microtome (Leica Biosystems, Deer Park, Illinois, USA, RM2255) and mounted on albumin-coated slides. Deparaffinated slides were stained in filtered 0.2% toluidine blue (UCB, Brussels, Belgium) for several minutes, then rinsed with mQ water, air-dried and sealed with Entellan® new (Sigma-Aldrich, Merck KGaA, Darmstadt, Germany).

In situ hybridization

Sample fixation in FAA and embedding in paraffin were performed as described earlier, except that the slides were coated with 0.5% poly-L-lysine (Sigma-Aldrich, Merck KGaA, Darmstadt, Germany) dissolved in 16 mM Tris. After deparaffination and rehydration, an acidic hydrolysis of the tissues was performed with 0.2 M HCl for 30 min. It was followed by a 0.01% proteinase K treatment for 30 min at 37°C, stopped by 2 min in 0.2% glycine, 1× phosphate buffered saline (PBS) solution, and rinsing with 1× PBS. The tissues were re-fixated in 4% formaldehyde and 1× PBS for 10 min, then rinsed with 1× PBS and dehydrated with an EtOH series. Hybridization was subsequently performed as described in Lozano et al. (1998) and manufacturer's protocol ('DIG Application Manual for Nonradioactive In Situ Hybridization', 4th Edition, Roche).

For probe synthesis, *SP* (Solyc06g074350), *BRC1a* (Solyc03g119770) and *BRC1b* (Solyc06g069240) coding sequences were amplified by PCR (primers in **Supplementary Table S2**) using cDNA from young inflorescences (AC accession) as the template and the resulting products were cloned into pBlueScript vector (Addgene, Watertown, Massachusetts, USA). PCR synthesis was performed using the plasmid as the template and primers with the T7 promoter sequence (primers in **Supplementary Table S2**) to obtain linear DNA. Sense and antisense probes were synthesized with RNA T7 polymerase (Promega) and DIG-labeled nucleotides for 2 h at 37°C. The DNA template was eliminated with an RNase-free DNase treatment (Promega), and the probe quality, size and concentration were estimated on 1.5% agarose gel. RNA probes were chemically hydrolyzed to ∼120-b fragments by adding 30 μl of 200 mM Na_2CO_3 and 20 μl of 200 mM $NaHCO_3$ to 50 μl of RNA and incubating at 60°C. Hydrolysis time (t) was calculated as follows: $t = (L_0 - L_f)/(K \times L_0 \times L_f)$, where L_0 is the initial length of the RNA probe (kb), L_f is the final length of RNA probe (0.12 kb) and K is the constant rate (0.11 kb/min). After hydrolysis, RNA probes were purified by precipitation overnight at −20°C and diluted in water. Preliminary experiments performed with the *BRC1a* and *BRC1b* probes revealed very weak expression levels; we thus decided to use a mixture of the two probes to increase the signal-to-noise ratio.

Supplementary Data

Supplementary data are available at *PCP* online.

Data Availability

The author responsible for distribution of materials integral to the findings presented in this article is C.P. (cperilleux@uliege.be). The raw data of the RNA-seq experiments are available in the Sequence Read Archive (SRA) database of the National Center for Biotechnology Information (NCBI) (BioProject ID: PRJNA940640).

Funding

F.N.R.S. – F.R.I.A. (PhD grant 1.E.012.18 to S.H.-F.).

Acknowledgments

The authors would like to thank Prof. M. Hernould (University of Bordeaux, INRAE Bordeaux) for sharing his expertise in tomato plant transformation; they are also grateful to Denis Libion, Patricia Perruzza and Gabriel Berger for propagating and taking care of the plants. S. H.-F. is grateful to the F.R.I.A. for the award of a PhD fellowship.

Disclosures

The authors declare no conflict of interest.

References

Anders, S., Pyl, P.T. and Huber, W. (2015) HTSeq—a Python framework to work with high-throughput sequencing data. *Bioinformatics* 31: 166–169.

Barbier, F.F., Dun, E.A., Kerr, S.C., Chabikwa, T.G. and Beveridge, C.A. (2019) An update on the signals controlling shoot branching. *Trends Plant Sci.* 24: 220–236.

Berbel, A., Ferrandiz, C., Hecht, V., Dalmais, M., Lund, O.S., Sussmilch, F.C., et al. (2012) VEGETATIVE1 is essential for development of the compound inflorescence in pea. *Nat. Commun.* 3: 797.

Bergougnoux, V. (2014) The history of tomato: from domestication to biopharming. *Biotechnol. Adv.* 32: 170–189.

Bolger, A.M., Lohse, M. and Usadel, B. (2014) Trimmomatic: a flexible trimmer for Illumina sequence data. *Bioinformatics* 30: 2114–2120.

Boumlik, R., Bendahmane, A. and Gomez-Roldan, M.V.G. (2021) MIKC-type MADS-box transcription factors in tomato reproductive development: an overview of their role in meristems, flower, fruit, and flower abscission zone development. *Annu. Plant Rev. Online.* 4: 907–942.

Butler, L. (1936) Inherited characters in the tomato. II. Jointless pedicel. *J. Heredity* 27: 25–26.

Castaneda, L., Gimenez, E., Pineda, B., Garcia-Sogo, B., Ortiz-Atienza, A., Micol-Ponce, R., et al. (2022) Tomato CRABS CLAW paralogues interact with chromatin remodelling factors to mediate carpel development and floral determinacy. *New Phytol.* 234: 1059–1074.

Castel, R., Kusters, E. and Koes, R. (2010) Inflorescence development in petunia: through the maze of botanical terminology. *J. Exp. Bot.* 61: 2235–2246.

Cheng, X., Li, G., Tang, Y. and Wen, J. (2018) Dissection of genetic regulation of compound inflorescence development in Medicago truncatula. *Development.* 145: dev158766.

de Martino, G., Pan, I., Emmanuel, E., Levy, A. and Irish, V.F. (2006) Functional analyses of two tomato APETALA3 genes demonstrate diversification in their roles in regulating floral development. *Plant Cell* 18: 1833–1845.

Emery, G.C. and Munger, H.M. (1970) Alteration of growth and flowering in tomatos by the jointless genotype. *J. Heredity* 61: 51–53.

Gimenez, E., Castaneda, L., Pineda, B., Pan, I.L., Moreno, V., Angosto, T., et al. (2016) TOMATO AGAMOUS1 and ARLEQUIN/TOMATO AGAMOUS-LIKE1 MADS-box genes have redundant and divergent functions required for tomato reproductive development. *Plant Mol. Biol.* 91: 513–531.

Gomez-Roldan, M.V.G., Périlleux, C., Morin, H., Huerga-Fernández, S., Latrasse, D., Benhamed, M., et al. (2017) Natural and induced loss of function mutations in SlMBP21 MADS-box gene led to jointless-2 phenotype in tomato. *Sci. Rep*. 7: 4402.

Gross, T., Broholm, S. and Becker, A. (2018) CRABS CLAW acts as a bifunctional transcription factor in flower development. *Front. Plant Sci*. 9: 835.

He, C. and Saedler, H. (2005) Heterotopic expression of MPF2 is the key to the evolution of the Chinese lantern of Physalis, a morphological novelty in Solanaceae. *Proc. Natl. Acad. Sci. U.S.A*. 102: 5779–5784.

He, J., Alonge, M., Ramakrishnan, S., Benoit, M., Soyk, S., Reem, N.T., et al. (2023) Establishing Physalis as a Solanaceae model system enables genetic reevaluation of the inflated calyx syndrome. *Plant Cell* 35: 351–368.

Hileman, L.C., Sundstrom, J.F., Litt, A., Chen, M., Shumba, T. and Irish, V.F. (2006) Molecular and phylogenetic analyses of the MADS-box gene family in tomato. *Mol. Biol. Evol*. 23: 2245–2258.

Jiang, X., Lubini, G., Hernandes-Lopes, J., Rijnsburger, K., Veltkamp, V., de Maagd, R.A., et al. (2022) FRUITFULL-like genes regulate flowering time and inflorescence architecture in tomato. *Plant Cell* 34: 1002–1019.

Karlova, R., Rosin, F.M., Busscher-Lange, J., Parapunova, V., Do, P.T., Fernie, A.R., et al. (2011) Transcriptome and metabolite profiling show that APETALA2a is a major regulator of tomato fruit ripening. *Plant Cell* 23: 923–941.

Kim, S., Soltis, P.S., Wall, K. and Soltis, D.E. (2006) Phylogeny and domain evolution in the APETALA2-like gene family. *Mol. Biol. Evol*. 23: 107–120.

Leseberg, C.H., Eissler, C.L., Wang, X., Johns, M.A., Duvall, M.R. and Mao, L. (2008) Interaction study of MADS-domain proteins in tomato. *J. Exp. Bot*. 59: 2253–2265.

Li, Z., Zeng, S., Li, Y., Li, M. and Souer, E. (2016) Leaf-like sepals induced by ectopic expression of a SHORT VEGETATIVE PHASE (SVP)-like MADS-box gene from the basal eudicot epimedium sagittatum. *Front. Plant Sci*. 7: 1461.

Lippman, Z.B., Cohen, O., Alvarez, J.P., Abu-Abied, M., Pekker, I., Paran, I., et al. (2008) The making of a compound inflorescence in tomato and related nightshades. *PLoS Biol*. 6: e288.

Litt, A. and Irish, V.F. (2003) Duplication and diversification in the APETALA1/FRUITFULL floral homeotic gene lineage: implications for the evolution of floral development. *Genetics* 165: 821–833.

Liu, D., Wang, D., Qin, Z., Zhang, D., Yin, L., Wu, L., et al. (2014) The SEPALLATA MADS-box protein SLMBP21 forms protein complexes with JOINTLESS and MACROCALYX as a transcription activator for development of the tomato flower abscission zone. *Plant J*. 77: 284–296.

Love, M.I., Huber, W. and Anders, S. (2014) Moderated estimation of fold change and dispersion for RNA-seq data with DESeq2. *Genome Biol*. 15: 550.

Lozano, R., Angosto, T., Gomez, P., Payan, C., Capel, J., Huijser, P., et al. (1998) Tomato flower abnormalities induced by low temperatures are associated with changes of expression of MADS-Box genes. *Plant Physiol*. 117: 91–100.

MacAlister, C.A., Park, S.J., Jiang, K., Marcel, F., Bendahmane, A., Izkovich, Y., et al. (2012) Synchronization of the flowering transition by the tomato TERMINATING FLOWER gene. *Nat. Genet*. 44: 1393–1398.

Maheepala, D.C., Emerling, C.A., Rajewski, A., Macon, J., Strahl, M., Pabon-Mora, N., et al. (2019) Evolution and diversification of FRUITFULL genes in Solanaceae. *Front. Plant Sci*. 10: 43.

Mao, L., Begum, D., Chuang, H.W., Budiman, M.A., Szymkowiak, E.J., Irish, E.E., et al. (2000) JOINTLESS is a MADS-box gene controlling tomato flower abscission zone development. *Nature* 406: 910–913.

Martin-Trillo, M., Grandio, E.G. Serra, F., Marcel, F., Rodriguez-Buey, M.L., Schmitz, G., et al. (2011) Role of tomato BRANCHED1-like genes in the control of shoot branching. *Plant J*. 67: 701–714.

Meir, Z., Aviezer, I., Chongloi, G.L., Ben-Kiki, O., Bronstein, R., Mukamel, Z., et al. (2021) Dissection of floral transition by single-meristem transcriptomes at high temporal resolution. *Nat. Plants* 7: 800–813.

Nakano, T., Kimbara, J., Fujisawa, M., Kitagawa, M., Ihashi, N., Maeda, H., et al. (2012) MACROCALYX and JOINTLESS interact in the transcriptional regulation of tomato fruit abscission zone development. *Plant Physiol*. 158: 439–450.

Park, S.J., Jiang, K., Schatz, M.C. and Lippman, Z.B. (2012) Rate of meristem maturation determines inflorescence architecture in tomato. *Proc. Natl. Acad. Sci. U.S.A*. 109: 639–644.

Périlleux, C. and Huerga-Fernández, S. (2022) Reflections on the triptych of meristems that build flowering branches in tomato. *Front. Plant Sci*. 13: 798502.

Périlleux, C., Lobet, G. and Tocquin, P. (2014) Inflorescence development in tomato: gene functions within a zigzag model. *Front. Plant Sci*. 5: 121.

Philouze, J. (1978) Comparaison des effets des gènes j et j-2 conditionnant le caractère "jointless" chez la Tomate et relations d'épistasie entre j et j-2 dans des lignées de même type variétal. *Ann. Amél. Plantes* 28: 431–445.

Pineda, B., Gimenez-Caminero, E., Garcia-Sogo, B., Anton, M.T., Atares, A., Capel, J., et al. (2010) Genetic and physiological characterization of the arlequin insertional mutant reveals a key regulator of reproductive development in tomato. *Plant Cell Physiol*. 51: 435–447.

Pnueli, L., Carmel-Goren, L., Hareven, D., Gutfinger, T., Alvarez, J., Ganal, M., et al. (1998) The SELF-PRUNING gene of tomato regulates vegetative to reproductive switching of sympodial meristems and is the ortholog of CEN and TFL1. *Development* 125: 1979–1989.

Quinet, M., Bataille, G., Dobrev, P.I., Capel, C., Gomez, P., Capel, J., et al. (2014) Transcriptional and hormonal regulation of petal and stamen development by STAMENLESS, the tomato (Solanum lycopersicum L.) orthologue to the B-class APETALA3 gene. *J. Exp. Bot*. 65: 2243–2256.

Quinet, M., Dubois, C., Goffin, M.C., Chao, J., Dielen, V., Batoko, H., et al. (2006) Characterization of tomato (Solanum lycopersicum L.) mutants affected in their flowering time and in the morphogenesis of their reproductive structure. *J. Exp. Bot*. 57: 1381–1390.

Rick, C.M. and Butler, L. (1956) Cytogenetics of the tomato. *Adv. Genet*. 8: 267–382.

Rick, C.M. and Sawant, A.C. (1955) Factor interactions affecting the phenotypic expression of the jointless character in tomatoes. *Proc. Amer. Soc. Hort. Sci* 66: 354–360.

Satoh-Nagasawa, N., Nagasawa, N., Malcomber, S., Sakai, H. and Jackson, D. (2006) A trehalose metabolic enzyme controls inflorescence architecture in maize. *Nature* 441: 227–230.

Shalit, A., Rozman, A., Goldshmidt, A., Alvarez, J.P., Bowman, J.L., Eshed, Y., et al. (2009) The flowering hormone florigen functions as a general systemic regulator of growth and termination. *Proc. Natl. Acad. Sci. U.S.A*. 106: 8392–8397.

Soyk, S., Lemmon, Z.H., Oved, M., Fisher, J., Liberatore, K.L., Park, S.J., et al. (2017) Bypassing negative epistasis on yield in tomato imposed by a domestication gene. *Cell* 169: 1142–1155 e1112.

Szymkowiak, E.J. and Irish, E.E. (2006) JOINTLESS suppresses sympodial identity in inflorescence meristems of tomato. *Planta* 223: 646–658.

Tabuchi, T., Ito, S. and Arai, N. (2000) Development of the abscission zones in *j-2in* pedicels of galapagos wild tomatoes. *J. Jpn. Soc. Hortic. Sci* 69: 443–445.

Thouet, J. (2011) Contribution à l'étude du contrôle génétique de la croissance sympodiale et de l'architecture inflorescentielle chez la tomate. PhD thesis, University of Liège

Thouet, J., Quinet, M., Lutts, S., Kinet, J.M., Périlleux, C. and Blazquez, M.A. (2012) Repression of floral meristem fate is crucial in shaping tomato inflorescence. *PLoS One* 7: e31096.

Thouet, J., Quinet, M., Ormenese, S., Kinet, J.M. and Périlleux, C. (2008) Revisiting the involvement of SELF-PRUNING in the sympodial growth of tomato. *Plant Physiol.* 148: 61–64.

Vrebalov, J., Ruezinsky, D., Padmanabhan, V., White, R., Medrano, D., Drake, R., et al. (2002) A MADS-box gene necessary for fruit ripening at the tomato ripening-inhibitor (rin) locus. *Science* 296: 343–346.

Wang, M., Le Moigne, M.A., Bertheloot, J., Crespel, L., Perez-Garcia, M.D., Oge, L., et al. (2019a) BRANCHED1: a key hub of shoot branching. *Front. Plant Sci.* 10: 76.

Wang, Y., Zhang, J., Hu, Z., Guo, X., Tian, S. and Chen, G. (2019b) Genome-wide analysis of the MADS-box transcription factor family in Solanum lycopersicum. *Int. J. Mol. Sci.* 20: 2961.

Yant, L., Mathieu, J., Dinh, T.T., Ott, F., Lanz, C., Wollmann, H., et al. (2010) Orchestration of the floral transition and floral development in Arabidopsis by the bifunctional transcription factor APETALA2. *Plant Cell* 22: 2156–2170.

Yuste-Lisbona, F.J., Quinet, M., Fernandez-Lozano, A., Pineda, B., Moreno, V., Angosto, T., et al. (2016) Characterization of vegetative inflorescence (mc-vin) mutant provides new insight into the role of MACROCALYX in regulating inflorescence development of tomato. *Sci. Rep.* 6: 18796.

Zhang, H.B., Budiman, M.A. and Wing, R.A. (2000) Genetic mapping of jointless-2 to tomato chromosome 12 using RFLP and RAPD markers. *Theor. Appl. Genet.* 100: 1183–1189.

Zhang, Z., Coenen, H., Ruelens, P., Hazarika, R.R., Al Hindi, T., Oguis, G.K., et al. (2018) Resurrected protein interaction networks reveal the innovation potential of ancient whole-genome duplication. *Plant Cell* 30: 2741–2760.

Zhao, J., Tian, Y., Zhang, J.S., Zhao, M., Gong, P., Riss, S., et al. (2013) The euAP1 protein MPF3 represses MPF2 to specify floral calyx identity and displays crucial roles in Chinese lantern development in Physalis. *Plant Cell* 25: 2002–2021.

Plant Cell Physiol. 00(00): 1–15 (2024) doi:https://doi.org/10.1093/pcp/pcae046, Advance Access publication on 18 April 2024, available online at https://academic.oup.com/pcp